SPHERICAL BLAST WAVES IN MULTICOMPONENT MEDIA

G. M. Lyakhov and V. N. Okhitin

UDC 624.131.43.539.215

The solution of the problem of propagation of a wave in soils is presented for the case when the wave is produced by the detonation of a spherical charge of some explosive material (EM). The solution is obtained on a computer by the method of characteristics. The soils are regarded as multicomponent media consisting of solid particles, water, and air in conformity with the model proposed in [1, 2]. The dependence of the pressure, velocity of the particles, and the density in the wave front on the distance is determined; the variation of these parameters with time at fixed points of the medium is also determined. The results are compared with the results of tests [1, 2]. Their close agreement for different contents of the components indicates the applicability of the multicomponent model to soils. The limits of applicability of the model are determined. The propagation of a plane wave under the same conditions was investigated in [3].

1. Model of the Soil and the Scheme of the Process. Soils are multicomponent media having a rigid skeleton. Therefore two mechanisms of compression exist simultaneously. The first is related to the transmission of the load through the contacts among the solid grains, their displacement, and overpacking (compressibility of the skeleton); the second is related to the compressibility of air, water, and the material of the solid component (compressibility of the three-component medium). The effect of these mechanisms on the overall compressibility in different soils and in the same solid for different loads is different. For small loads the main reaction to the compression is offered by the skeleton. In these conditions the models of elastoplastic or viscoplastic media are used. For sufficiently large loads $p > p^*$, when the volumetric deformations far exceed the content of the gas component in the soil, the main reaction to the compression is offered by the soil as a multicomponent medium. The value of p^* depends significantly on the content of the components; p^* increases with the content of the gaseous components. In water-saturated soils with the gaseous content equal to thousandths of the volume p^* corresponds to several atmospheres; in unsaturated soils it corresponds to hundreds, thousands, and tens of thousand atmospheres.

According to the model of a multicomponent medium [1, 2] the deformations occur instantaneously at the instant of application of the load; the tangential stresses are negligibly small and the equations of compression and decompression are of the form

$$\frac{\rho_0}{\rho} = \alpha_1\left(\frac{p}{p_0}\right)^{-1/\gamma_1} + \alpha_2\left[\frac{\gamma_2(p-p_0)}{\rho_2 c_2^2}+1\right]^{-1/\gamma_2} + \alpha_3\left[\frac{\gamma_3(p-p_0)}{\rho_3 c_3^2}+1\right]^{-1/\gamma_3} \tag{1.1}$$

$$\alpha_1+\alpha_2+\alpha_3=1, \quad \rho_0=\alpha_1\rho_1+\alpha_2\rho_2+\alpha_3\rho_3$$

where α_1, α_2, α_3 are the volume contents of air, water, and the solid component, ρ_1, ρ_2, ρ_3 are their densities, c_1, c_2, c_3 are the speeds of sound in them, and is the density of the three-component medium. All these quantities are referred to atmospheric pressure p_0.

Different schemes of explosion are used in the solution of wave problems. At the initial a spherical detonation wave appears at the center of the spherical charge, which is reflected from the boundary with the medium. Later the motion of converging and diverging compression and rarefaction waves occurs through the products of detonation. These processes are usually not taken into consideration; the detonation is taken to be instantaneous and the expansion of the detonation products is taken to occur according to the isentropic law [4, 5]. At a sufficient distance from the point of detonation with the maximum pressure

Moscow. Translated from Prikladnoi Mekhaniki i Tekhnicheskoi Fiziki, No. 2, pp. 75-84, March-April, 1974. Original article submitted May 29, 1973.

TABLE 1

Medium No.	α_1	α_2	α_3
1	0	0.4	0.6
2	0.0005	0.3995	0.6
3	0.01	0.39	0.6
4	0.02	0.38	0.6
5	0.04	0.36	0.6
6	0	1	0

of the order of thousand atmospheres and smaller the wave parameters in this approach are practically the same as in the more complex scheme taking into consideration the wave processes in the detonation. We shall make use of this scheme.

In accordance with [6] we assume that the isentropic equation of the detonation products is of the form

$$p = A\rho^n + B\rho^{\gamma+1} \tag{1.2}$$

At large and small pressures (1.2) goes over respectively into the equations [7]

$$p = p_n(\rho/\rho_n)^{k_n} \tag{1.3}$$

$$p = p_0(\rho/\rho_0)^{k_0} \tag{1.4}$$

The pressure p_n and density ρ_n correspond to the instantaneous detonation; p_0 and ρ_0 correspond to the atmospheric pressure.

The quantities A, B, n, and γ are determined from the conditions that curves (1.2) and (1.3) must have a common point $p_n\rho_n$ and a common tangent at this point, and also that curves (1.2) and (1.4) must have a common tangent for $\rho \to 0$; in expansion from $p_n\rho_n$ the detonation products do work equal to the heat of the explosive conversion Q.

From these conditions and (1.2) we obtain a system of four equations for A, B, N, γ:

$$\begin{aligned} k_n &= n + \frac{B\rho^{\gamma+1}}{p_n}(\gamma + 1 - n), \quad \gamma = k_0 - 1 \\ Q &= \frac{p_n}{\rho_n(n-1)} + \frac{B\rho_n^{\gamma}}{\gamma(n-1)}(n - \gamma - 1) \end{aligned} \tag{1.5}$$

We shall use Lagrangian variables: r – the spatial coordinate, t – time. In these variables the basic equations of motion are of the form

$$\frac{\partial V}{\partial t} + \frac{1}{\rho_0}\left(\frac{R}{r}\right)^{\nu}\frac{\partial u}{\partial r} = \frac{\nu u V}{R}, \quad \frac{\partial u}{\partial t} + \frac{1}{\rho_0}\left(\frac{R}{r}\right)^{\nu}\frac{\partial p}{\partial r} = 0, \quad \frac{\partial R}{\partial t} = u, \quad V = \frac{1}{\rho} \tag{1.6}$$

Here R is Euler coordinate, $\nu = 2$.

System (1.6) has two families of characteristics

$$\begin{aligned} &\frac{dp}{\rho c} + du + \frac{\nu u c}{R}dt = 0 \quad \text{for} \quad dr = \frac{c\rho}{\rho_0}\left(\frac{R}{r}\right)^{\nu}dt \\ &\frac{dp}{\rho c} - du + \frac{\nu u c}{R}dt = 0 \quad \text{for} \quad dr = -\frac{c\rho}{\rho_0}\left(\frac{R}{r}\right)^{\nu}dt \end{aligned} \tag{1.7}$$

System (1.6) is closed by Eq. (1.1). The boundary conditions at the contact discontinuity T, i.e., for $r = r_0$ and at the shock wave front are

$$\rho/\rho_n = (r_0/R)^3 \tag{1.8}$$

$$p - p_0 = \rho_0 u D, \quad (\rho - \rho_0)D = \rho u \tag{1.9}$$

We pass on to dimensionless quantities and dimensionless Lagrangian variables

$$\begin{aligned} &p^\circ = p/p_n, \ \rho^\circ = \rho/\rho_n, \ c^\circ = c/c_n, \ u^\circ = u/c_n \\ &D^\circ = D/c_n, \ R^\circ = R/r_0, \ x = r/r_0, \ \tau = tc_n/r_0 \end{aligned} \tag{1.10}$$

where r_0 is the radius of the charge of EM.

In the new variables the isentropic equation (1.2) of the detonation products becomes

$$p^\circ = A^\circ(\rho^\circ)^n + B^\circ(\rho^\circ)^{\gamma+1}, \ A^\circ = A\rho_n^n/p_n, \quad B^\circ = B\rho_n^{\gamma+1}/p_n \tag{1.11}$$

The quantities A°, B°, n, γ are determined from equations that follow from (1.5) and (1.2)

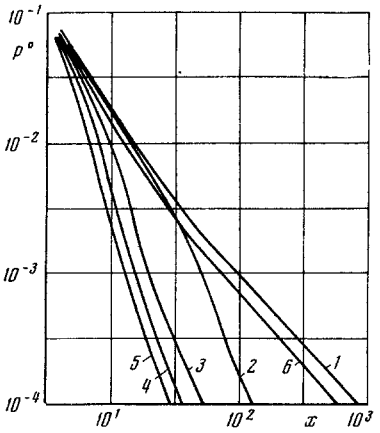

Fig. 1

$$A^\circ + B^\circ = 1, \quad k_n = n + B^\circ(\gamma - n + 1), \quad \gamma = k_0 - 1$$

$$Q^\circ = \frac{Qp_n}{p_n} = \frac{1}{n-1} + \frac{B^\circ}{\gamma(n-1)}(n - \gamma - 1)$$

The boundary conditions at the wave front are

$$\rho^\circ = (R^\circ)^{-3} \quad \text{for} \quad x = 1$$
$$p^\circ - p_0^\circ = k_n\rho_0^\circ D^\circ u^\circ, \quad (\rho^\circ - \rho_0^\circ) D^\circ = p^\circ u^\circ \tag{1.12}$$

In the dimensionless form the equation of compressibility of a multicomponent medium is

$$\frac{\rho_0^\circ}{\rho^\circ} = \alpha_1\left(\frac{p^\circ}{p_0^\circ}\right)^{-1/\gamma_1} + \alpha_2\left[\frac{\gamma_2(p^\circ - p_0^\circ)}{k_n\rho_2^\circ c_2^{\circ 2}} + 1\right]^{-1/\gamma_2} +$$
$$\alpha_3\left[\frac{\gamma_3(p^\circ - p_0^\circ)}{k_n\rho_3^\circ c_3^{\circ 2}} + 1\right]^{-1/\gamma_3} \tag{1.13}$$

The characteristic equations are

$$\frac{dp^\circ}{k_n\rho^\circ c_0^\circ} \pm du^\circ + \frac{\nu u^\circ c^\circ}{R^\circ} d\tau = 0 \quad \text{for} \quad dx = \pm \frac{c^\circ\rho^\circ}{\rho_0^\circ}\left(\frac{R^\circ}{x}\right) d\tau \tag{1.14}$$

The problem was solved for a trotyl-type EM, five water-saturated soils with different contents of the gaseous component and water. The computed characteristics of the EM and the media are given in Table 1 for $k_n = 3$, $k_0 = 1.25$, $p_n = 96{,}000$ kg/cm^2, $\rho_n = 1.6$ g/cm^3, $Q = 1000$ cal/g.

The porosity of the soils was identical, $n = 0.4$, $\rho_1 = 12 \cdot 10^{-4}$ g/cm^3, $\rho_2 = 1$ g/cm^3, $\rho_3 = 2.65$ g/cm^3, $c_1 = 330$ m/sec, $c_2 = 1500$ m/sec, $c_3 = 4500$ m/sec, $\gamma_1 = 1.4$, $\gamma_2 = 7$, $\gamma_3 = 4$. Here $n = \alpha_1 + \alpha_2$.

In the investigated problem the plane $x\tau$ contains three types of points (at each of these the parameters are computed according to separate algorithms): at the shock wave front S, in the medium between S and the contact discontinuity T, and at the contact discontinuity T.

The step Δx along the spatial coordinate was taken constant. The magnitude of the step depends on the required accuracy of the computation. The step in time varies from layer to layer in accordance with the scheme [8].

We consider the sequence of the computation of the parameters at the front S. Let points A and B lie on a single time layer. The parameters at these points are unknown. Points B and K lie in the shock front. The parameters at K are determined. For starting the computation the parameters p° and u° of point B are carried over to point K. Then the characteristic is drawn from K to the preceding time layer. We denote the point of its intersection with line AB by L. The coordinate of this point is

$$x_L = x_K - \left[\frac{c^\circ\rho^\circ}{\rho_0^\circ}\left(\frac{R^\circ}{x}\right)^\nu\right]_{KL}\Delta\tau, \quad R_K^\circ = x_K = R_B^\circ + \Delta x$$

The index KL indicates that the quantities in the brackets take average values between K and L. In the first computation they coincide at point K. The quantities p_L°, u_L°, R_L° are determined from the coordinate x_L by interpolation over the parameters at points A and B. Here $\rho^\circ = \rho^\circ(p_L)$, $c_L^\circ = c^\circ(\rho_L)$.

The refined values u°, p°, D°, and ρ° at point K are obtained from p_L°, u_L°, R_L° using the equations at the shock wave front and the condition satisfied at the characteristic

$$p_K^\circ - p_0^\circ = k_n\rho_0^\circ D_K^\circ u_K^\circ, \quad (\rho_K^\circ - \rho_0^\circ) D_K^\circ = \rho_K^\circ u_K^\circ$$
$$[1/k_n\rho^\circ c^\circ]_{KL}(p_K^\circ - p_L^\circ) + (u_K^\circ - u_L^\circ) - [\nu u^\circ c^\circ / R^\circ]_{KL}\Delta\tau = 0$$

Together with (1.13) we obtain a system of four equations for the four unknowns.

The computation was repeated a given number of times for refining the results.

The computation at the other types of points is done in a similar way, starting from the characteristic equations in the medium and Eqs. (1.8) and (1.11) at the contact discontinuity.

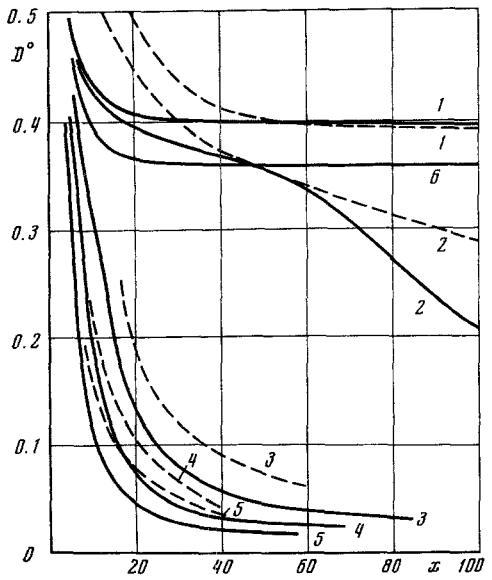

Fig. 2

2. Results of Computation. Let us consider the parameters at the shock front. The graphs of the dimensionless quantities, i.e., the pressure and the velocity of the front, are shown in Figs. 1-2. Here and below the numbering of the curves corresponds to the sequence of the media in Table 1. The computed graphs are shown by continuous lines, the experimental by dashes. It follows from a comparison of the curves in Fig. 1 that the rate of decay of the maximum pressure with the distance increases substantially with the increase in the content of the gaseous component in the soil. For $\alpha_1 = 0.04$ the pressure at a sufficient distance from the point of explosion is almost two orders of magnitude smaller than for $\alpha_1 = 0$. In water (graph 6) the pressure decays more rapidly than in the soil with $\alpha_1 = 0$, but considerably less rapidly than in media containing air.

The dependence of the velocity of the wave front D° on the distance is shown in Fig. 2. The rate of decrease of the velocity increases considerably with the increase in the air content: the most intense change in D° in all media occurs close to the point of explosion. Later the decrease of the velocity slows down considerably and its dimensional value gradually approaches the speed of sound c given by the equation that follows from (1.1)

$$c_0^2 = \frac{1}{\rho_0}\left(\frac{\alpha_1}{\rho_1 c_1^2} + \frac{\alpha_2}{\rho_2 c_2^2} + \frac{\alpha_3}{\rho_3 c_3^2}\right)^{-1} \qquad (2.1)$$

For n=0.4 and α_1 respectively equal to 0, 0.005, 0.01, 0.02, 0.04 the values of c_0 are 1620, 355, 85, 58, and 41 m/sec. For $\alpha_1 = 0$ the velocity D differs from c_0 by several percents even at a distance $x \sim 30$; for $\alpha_1 = 0.04$ the difference starts at larger distances ($x \sim 100$).

The computations show that the rate of decrease of the particle velocity u° does not increase monotonically with α_1, as in the case of D°. At small distances u° decreases with increasing α_1, but later the curves u° (x) corresponding to different air content may intersect. Thus, for x=10 u° is larger in the medium with $\alpha_1 = 0.01$ than in the medium with $\alpha_1 = 0.04$; for $x > 10$ the reverse situation is observed. For $x < 86$ the velocity in the medium with $\alpha_1 = 0.0005$ is greater than in the medium with $\alpha_1 = 0.04$; for $x > 86$ the dependence becomes reverse. In water the velocity of particles is larger than in other media. A similar nature of variation of u° is observed also in the case of plane waves [3].

Let us consider the variation of the parameters with time at fixed points of the medium. The graphs of p° (τ) and u° (τ) at points with coordinates x equal to 11.1 and 37 are shown in Figs. 3 and 4. It follows from the graphs that with the increase in α_1 the pressure decreases not only at the wave front but also behind the front. Thus, for example, in media with $\alpha_1 = 0.01$ and 0.04 the pressure at the front close to the point of explosion differs by a factor of 10, while for $\tau > 200$ it differs only by a few percent.

For a comparison of the rates of decay of the pressure behind the front in different media we introduce a quantity θ_* which is equal to the time in which the pressure at a fixed point decreases by a factor e; the corresponding dimensionless quantity is $\theta_*^\circ = \theta_n c_n / r_0$. In all media θ_*° increases with the distance from the point of explosion. The rate of increase of θ_*° with the increase in the air content also increases. For $\alpha_1 = 0$ and x=7.64, 19.11, 50, and 300 the values of θ_*° are 4.9, 7.9, 11.4, and 19.5 respectively. For $\alpha_1 = 0.01$ and x=8.25, 10, 20, 30, 50 θ_*° =5.5, 6.7, 9.3, 280, and 1000 respectively. For $\alpha_1 = 0.04$ and x=4, 7.69, 17.6, and 30 θ_*° =3, 18.5, 206, 820. The dependence θ_*° (x) is shown in Fig. 5. Graphs 6 is constructed from the experimental data for water [9]. The computed graph for water is not shown, since it practically coincides with 6. (For x=4, 10, 21, 26.9, 120, and 300 the obtained values are θ_*° = 2.4, 4.8, 8, 12.5, 19.1.)

The increase in the content of the gaseous component leads to a significant decrease of the rate of pressure decrease behind the wave front and to an increase of θ_*°. The values of θ_*° practically coincide in water and a two-component medium.

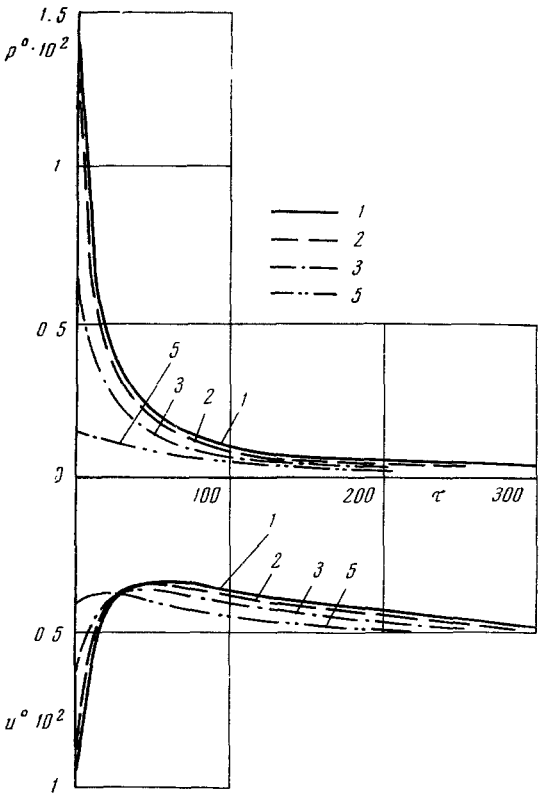

Fig. 3

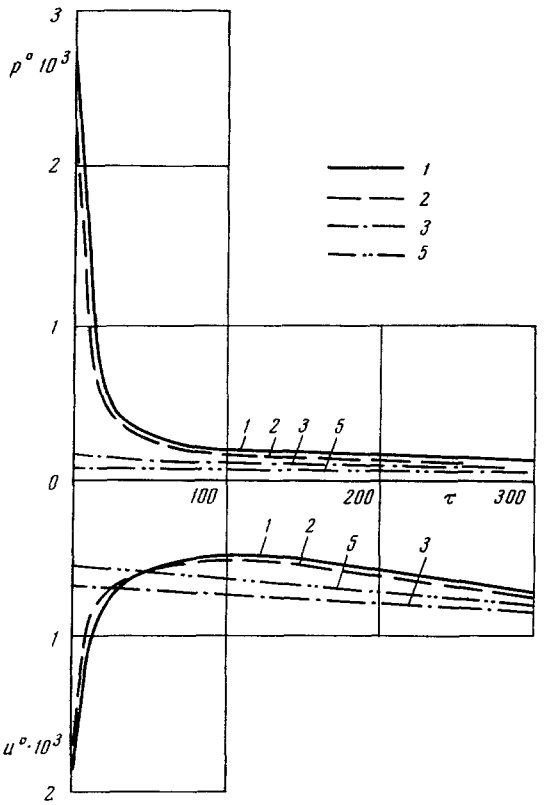

Fig. 4

The velocity of particles behind the wave front (Figs. 3 and 4) at points located at small distances (x=11.1) at first decreases with the passage of time and then slightly increases. For x=37 this dependence is retained in the case $\alpha_1=0$ and 0.005, but in media with large air content the increase of the velocity begins immediately behind the front. With time the velocities of the particles in all media become equal.

In an explosion a flux appears propagating from the gas chamber. Its velocity decreases with distance in all media, but at fixed points it may both increase and decrease with the time. Later on the velocity of the flux begins to decrease as a result of decrease of the dimensions of the gas chamber.

In the investigated media the change of pressure behind the wave front can be approximately described by the equations

$$\begin{aligned} p^\circ &= p_m^\circ e^{-\tau/\theta_*^\circ} \quad \text{for} \quad \tau \leqslant \theta_*^\circ \\ p^\circ &= p_m^\circ \theta_*^\circ / e\tau \quad \text{for} \quad \tau \geqslant \theta_*^\circ \end{aligned} \tag{2.2}$$

where τ is the time reckoned from the instant of arrival of the front at the investigated point and p_m° is the pressure at the wave front.

The graphs constructed from these equations practically coincide with the computed graphs in all media with $\alpha_1 \leq 0.005$. The difference in the curves increases with increasing α_1.

A comparison of the wave parameters in water and in a two-component medium (quarts) shows that the presence of solid particles in water causes an increase in the pressure and the velocity of the wave front, and a decrease of the velocity of the particles. Physically this is explained by the decrease of compressibility of the medium and the increase of its density.

The inclusion of the gaseous component does not significantly reduce the density but increases the compressibility significantly. This results in an increase of the curvature of the compression diagram and an increase of the losses in the shock front.

3. Comparison of Computational and Experimental Results. The process of dynamic deformation of a medium consisting of a solid frame, whose pores are filled with liquid and fine gas bubbles, is complex. In the investigation model it is assumed that the propagation of the blast waves is primarily determined by

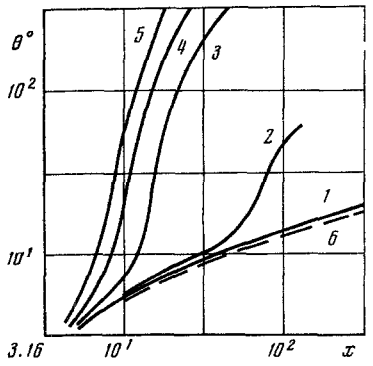

Fig. 5

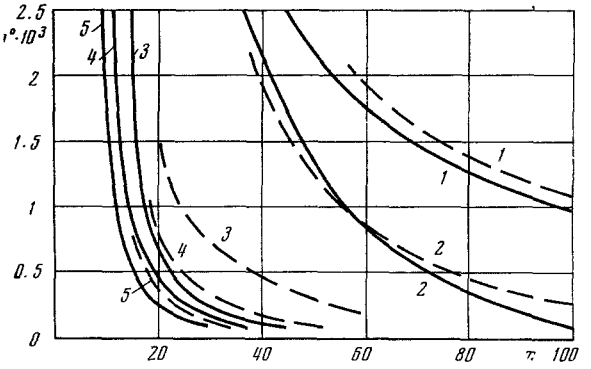

Fig. 6

the percent content of the components and their compressibility. Furthermore, it is possible to consider the difference in the velocities of displacement of the components and the stresses in them, the percent content of gas bubbles of different radius, the surface tension, the compressibility of the frame, the presence of tangential stresses in the frame, the phase transitions in the solid component, the change of temperature during the shock compression, and so forth. The effect of some of these factors is investigated in [10-14]. Their inclusion leads to an extreme complication of the model, which does not enable one to solve the explosion problem in these premises.

The purpose of the comparison of the computational and experimental results is to determine the applicability of the investigated model to water-saturated soils, where the content of the gaseous component is small and usually does not exceed 4-5% of the total volume.

The graphs of the dependence of the pressure in the wave front on the distance are shown in Fig. 6. The continuous lines pertain to computations and the dashes to experimental data. The experiments [2] were conducted for camouflet explosions of concentrated trotyl charges with 1.6, 5, and 40 kg weight in water-saturated sandy soils (curves 1, 2, 3, 5) and of charges with 5 and 25 kg weight in water-saturated clay soils (curve 4). The porosity of the sandy soils was $n \sim 0.4$, of clay $n \sim 0.2$. The media were finely dispersed; the radius of the gas bubbles ranged from 0 to 0.05 cm.

The content of trapped air in the same test areas was not identical. The deviations reached 50% of the mean value. The values of α_1 for the computations were taken from the mean values.

There is a good agreement between the behavior of the experimental and computational curves. The divergence of graphs 3 and 4 is somewhat larger than in other media, which should be explained by the possible exceedance of the true values as compared to the values used in the computations. For the soil with $\alpha_1 = 0.02$ the value of n taken in the computations is $n = 0.4$. Actually the soil was denser ($n = 0.2$). This also must result in a difference in the graphs. The divergence of the experimental and computed graphs in soils containing air increases with the distance from the point of explosion. In all cases the experimental results are higher than the computations.

The dependence of the velocity of the wave front on the distance is shown in Fig. 2. As in the case of the pressure the computed and experimental curves are in agreement. The computed values of D tend to the computed value of the speed of sound with increasing distance. For $\alpha_1 \geq 0.01$ the experimental values of D do not go below 150-200 m/sec, which corresponds to the velocity determined by the compressibility of the frame of the soil.

A comparison of the computed and experimental values of shows that there is a good agreement in soils with $\alpha_1 \leq 0.0005$. As α_1 increases the experimental values of $\theta_*°$ increase but to a smaller extent than the computed values. The difference increases with the distance from the point of explosion. For the largest value $\alpha_1 = 0.04$ at a distance $x = 20$ the computed value is 290, while the experimental value is ~ 200; at $x = 30$ the computed value is 820, while the experimental value is ~ 380.

According to the computations the wave remains a shock wave in all media at all distances. In the experiments in media with $\alpha_1 \geq 0.01$ the shock wave turns into a continuous compression wave as the distance from the point of explosion increases. For C = 5 kg a noticeable smearing of the jump is observed in medium with $\alpha_1 = 0.01$ at a distance $x = 45$, and in the medium with $\alpha_1 = 0.04$ at $x = 20$.

It follows from the comparison of the computed and experimental results that the investigated model reflects the basic physical characteristics of deformation of multicomponent media that are important for the propagation of blast waves. In a two-component medium (solid particles–water) and in a three-component medium with $\alpha_1 \leq 0.0005$ the computed and experimental values of the parameters practically coincide. A significant change in the pressure, the front velocity, and the velocity of the particles is observed (by one-two orders of magnitude) in the computations as well as in the experiments on increasing the content of the gaseous component. The decrease of the front velocity to 150-200 m/sec observed in the experiments with $\alpha_1 \leq 0.01$ and also the smaller decrease of the duration of the wave than in the computations are explained by the fact that at small pressures the total compressibility of the components in these media begins to exceed the compressibility of the frame.

As shown in [15], the smearing of the jump at the front and the conversion of the shock wave into a continuous compression wave are caused by the bulk viscosity of the medium; it follows from the model taking account of the viscous properties. In multicomponent media containing gas bubbles the viscous properties are primarily related to noninstantaneous compression of the bubbles under the action of the load, whose effect is particularly noticeable in the range of small pressures.

LITERATURE CITED

1. G. M. Lyakhov, "Shock waves in multicomponent media," Izv. Akad. Nauk SSSR, Otd. Tekl. Nauk. Mekhan. Mashinost., No. 1 (1959).
2. G. M. Lyakhov, Fundamentals of Dynamics of Explosions in Soils and Liquid Media [in Russian], Nedra, Moscow (1964).
3. G. M. Lyakhov, V. N. Okhitin, and A. G. Chistov, "Shock waves in soils and in water close to the point of explosion," Prikl. Mekhan. Tekl. Fiz., No. 3 (1972).
4. S. S. Grigoryan, "Solution of problem of underground explosion in soft soils," Prikl. Mat. Mekl., 28, No. 6 (1964).
5. P. Chadwick, A. Cox, and G. Hopkins, Mechanics of Deep Under-Ground Explosions [Russian translation] Mir, Moscow (1966).
6. L. V. Kashirskii, L. P. Orlenko, and V. N. Okhitin, "Effect of the equations of state on the dispersion of detonation products," Prikl. Mekhan. Tekl. Fiz., No. 2 (1973).
7. L. D. Landau and K. P. Stanyukovich, "On the study of detonation of concentrated explosive materials," Dokl. Akad. Nauk AN SSSR, 46, No. 9 (1945).
8. N. E. Hoskin, "Method of characteristics for solving equations of homogeneous nonsteady flow," in: Computational Methods in Hydrodynamics [Russian translation], Mir, Moscow (1967).
9. R. Kaul, Underwater Explosions, Dover (1965).
10. Kh. A. Rakhmatulin, "Fundamentals of gasdynamics of interpenetrating motions of compressible media," Prikl. Mat. Mekl., 20, No. 2 (1968).
11. G. K. Batcheler, "Compression waves in suspensions of gas bubbles," in: Mekhanika, No. 3 (1968).
12. V. N. Nikolaevskii, K. S. Basniev, A. T. Gorbunov, and G. A. Zotov, Mechanics of Saturated Porous Media [in Russian], Nedra, Moscow (1970).
13. R. I. Nigmatulin, "A model of the motion and shock waves in two-phase solid bodies with phase transitions," Prikl. Mekhan. Tekh. Fiz., No. 1 (1970).
14. G. F. Kopytov, "Damping of shock waves in a gas–liquid medium," Vestn. Leningr. Univ., No. 1 (1968).
15. G. M. Lyakhov and Ya. A. Pachetskii, "The role of viscous and plastic properties in the solution of wave problems," Prikl. Mekhan. Tekl. Fiz., No. 2 (1973).